ELSEVIER

Thermochimica Acta 396 (2003) 33–41

thermochimica acta

www.elsevier.com/locate/tca

The three reversible crystallization and melting processes of semicrystalline macromolecules☆

B. Wunderlich[a,b]

[a] *Department of Chemistry, University of Tennessee, Knoxville, TN 37996-1600, USA*
[b] *Oak Ridge National Laboratory, Chemical and Analytical Science Division, Oak Ridge, TN 37831-6197, USA*

Received 19 November 2001; received in revised form 15 June 2002; accepted 2 October 2002

Abstract

Linear, flexible macromolecules have long been recognized as being distributed between different metastable phases limited to micrometer and nanometer dimensions with their strong, covalent bonds crossing the phase boundaries. This structure leads to special properties and a multitude of changes are caused by differing thermal and mechanical histories. Temperature-modulated differential scanning calorimetry (TMDSC) and related thermal analysis techniques which can separate equilibrium and non-equilibrium responses within a sample are ideal for the analysis of such systems. A surprising observation in the last 5 years has been that there are some local, reversible ordering and disordering processes within this overall metastable aggregate. Three different reversible processes with latent heats have been identified and will be discussed using the example of polyethylene crystals: (1) The formation of larger concentrations of defects within the crystals. (2) The melting of small, paraffin-like crystals existing within the metastable arrangement. (3) The reversible, partial melting of chains at high-temperature which avoids molecular nucleation.
Published by Elsevier Science B.V.

Keywords: Temperature-modulated calorimetry; TMDSC; Melting; Semicrystalline polymers

1. Introduction

Semicrystalline polymers are microphase and nanophase structures. Fig. 1 contains a summary of such nanophases as given in the computer course "Thermal Analysis of Materials" (for details see the 36 lectures of the computer course [1]). Naturally, such a structure is not in equilibrium, complicating its thermodynamic description. Already the existence of more than one phase in a homopolymer at constant pressure over a wider temperature range indicates the absence of equilibrium, since the phase rule permits an equilibrium between two phases only at one, fixed transition temperature. In this paper, a summary is given of the experiments from our laboratory which help to develop insights into such semicrystalline samples with the help of temperature-modulated differential scanning calorimetry (TMDSC). A comprehensive review of this topic covering data on over 20 different semicrystalline polymers, analyzed by many different research groups, is in preparation for publication in 2002.

The variation of the enthalpy, dH, of a nanophase system at constant pressure can be followed by TMDSC. It is expressed by the change of enthalpy

☆ The submitted manuscript has been authored by a contractor of the US Government under the contract No. DOE-AC05-00OR22725. Accordingly, the US Government retains a non-exclusive, royalty-free license to publish or reproduce the published form of this contribution, or allow others to do so, for US Government purposes.

[1] *E-mail address:* wunderlich@chartertn.net (B. Wunderlich).

0040-6031/02/$ – see front matter. Published by Elsevier Science B.V.
PII: S0040-6031(02)00514-2

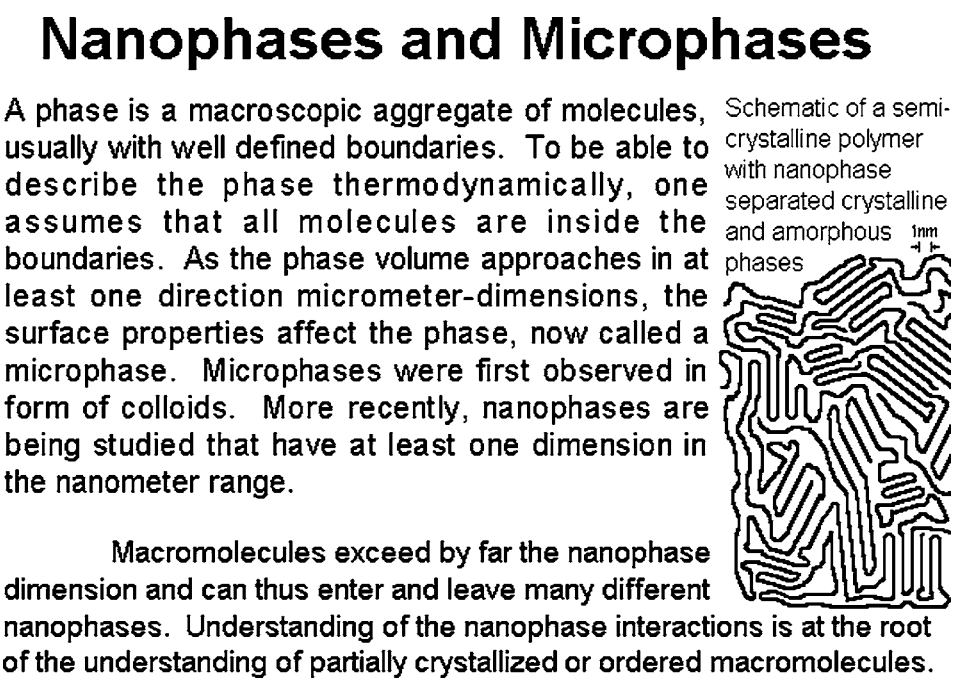

Fig. 1. Summary of phase definitions based on size, as given in the computer course "Thermal Analysis of Materials" [1].

with changing temperature, dT, which is given by the heat capacity, C_p, the differential of enthalpy with temperature at constant pressure, p, and composition, n ($C_p = (\partial H/\partial T)_{p,n}$ expressed in $\mathrm{J\,K^{-1}\,mol^{-1}}$) and its change during the progress of any possible transition, dn, at constant pressure and temperature, given by the latent heat as, for example on melting, by the heat of fusion, ΔH_f ($=(\partial H/\partial n)_{p,T}$, expressed in $\mathrm{J\,mol^{-1}}$):

$$\mathrm{d}H = C_p\,\mathrm{d}T + \Delta H_\mathrm{f}\,\mathrm{d}n \tag{1}$$

In Fig. 2, the vibrational C_p of polyethylene is illustrated along with a plot of the density of vibrational states [1]. This vibrational contribution will serve as the baseline for the discussion of the contributisons to H that may occur in the melting and crystallization ranges. Up to about 300 K, the skeletal and group vibrations are seen to account fully for the experimental C_p. Overall, the vibrations are the most important contributors to the enthalpy. Some 100 K below the equilibrium melting temperature, T_m^0 (=424.6 K), however, the experimental C_p starts to deviate from the vibrational contributions (total C_p in Fig. 2). The additional contribution to C_p arises from conformational motion [2], which in case of polyethylene is caused by the *gauche-trans* equilibrium which produces increasing numbers of local defects with temperature within the crystal. The vibrational and local conformational contributions are the two early recognized reversible contributions to the experimental heat capacity of polyethylene. Their time constant for the response to heating is in the femto- to picosecond range. Although not directly measurable with the DSC, its time constant can be judged from the upper plot in Fig. 2 [3]. Figs. 3 and 4 illustrate that the same increase beyond the total C_p of Fig. 2 occurs also for all normal paraffins, C_xH_{2x+2}, larger than propane, C_3H_5, at temperatures which are lower than the melting transitions [4].

The fully reversible vibrational and conformational contributions to C_p, as illustrated in Figs. 2–4, led to the development of the ATHAS data bank of heat capacities for polymers [5]. The introduction of temperature-modulated DSC in 1992 enabled a direct check of the reversibility of latent heat contributions in Eq. (1) which usually have much slower, cooperative kinetics. The seemingly reversible contribution

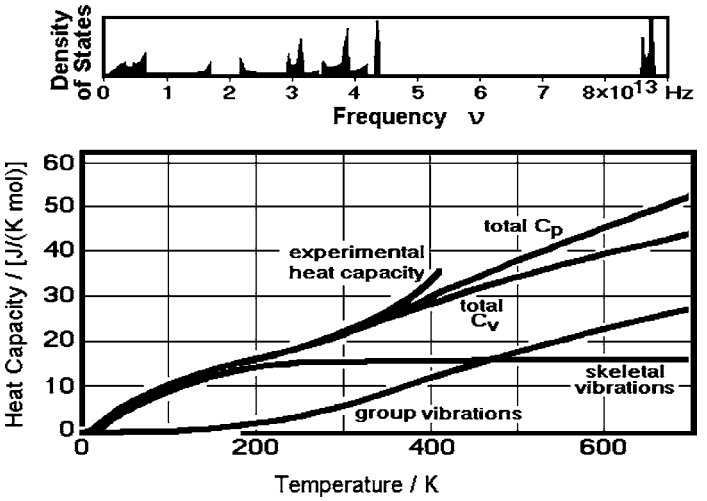

Fig. 2. Heat capacity of crystalline polyethylene and its contributions from the vibrations. The top graph represents the density of vibrational states as obtained by fitting a normal mode calculation to force constants from infrared and Raman spectra [2].

to melting in poly(ethylene terephthalate) (PET) displayed in Fig. 5 [6] was a surprising result, that needed further analysis since the directly measured kinetics of crystallization and melting monomers, oligomers, and polymers did not allow for a reverse melting in the range of modulation amplitudes of 0.1–3.0 K, typically used in TMDSC. In Fig. 6, plots of such crystallization and melting rates are shown [7]. Even when accounting for the fact that crystallization may form initially imperfect crystals (with a lower zero-entropy-production melting temperature), only rather short oligomer crystals should lead to reversing, and possibly even reversible melting. The term "reversing" is used to describe processes that appear in the reversing heat capacity of TMDSC which is equal to the modulus or absolute value of the complex heat capacity ($= |C_p^*|$) and evaluated from the first harmonic response of the heat-flow rate to the temperature modulation. After elimination or correction of all deviations that may have been introduced

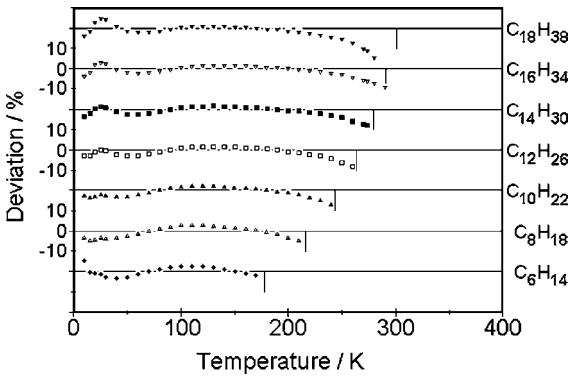

Fig. 3. Heat capacities of short-chain paraffins [4]. Shown is the difference of the calculated total heat capacity, as seen for polyethylene in Fig. 2, and the experimental heat capacity, indicating the increasing conformational contribution with temperature. The small vertical lines indicate transitions to the melt.

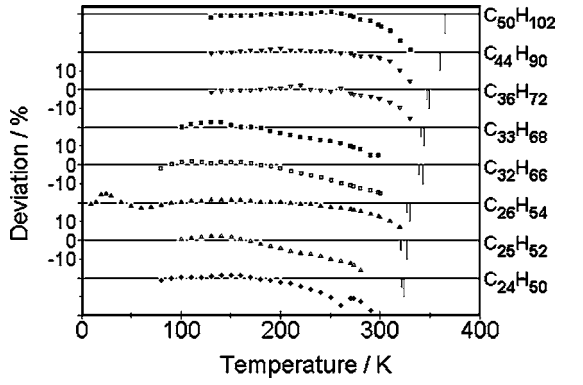

Fig. 4. Heat capacities of long-chain paraffins [4]. Shown is the difference of the calculated total heat capacity, as seen for polyethylene in Fig. 2, and the experimental heat capacity, indicating the increasing conformational contribution with temperature. The small vertical lines indicate transitions to the mesophases and the melt.

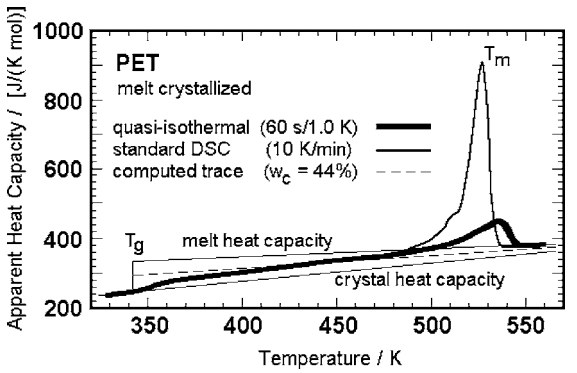

Fig. 5. Standard DSC and quasi-isothermal TMDSC of poly(ethylene terephthalate) (PET) [6]. The thin line represents the liquid and solid heat capacities, taken from the ATHAS data bank [5]. The dashed line is the heat capacity computed for the measured initial crystallinity of the sample. The glass transition temperature, T_g, and the melting peak temperature, T_m, are marked. The quasi-isothermal data points were taken every 2 K.

due to loss of steady state, linearity, and stationarity, as well as slowly changing metastable states on annealing, a process may be described as thermodynamically "reversible" [3]. The puzzle of reversible melting which should not occur in polymers represented by Fig. 6 will be addressed in this paper using our research results of TMDSC of flexible oligomers and polymers and the concept of molecular nucleation which requires a flexible-chain molecule to go

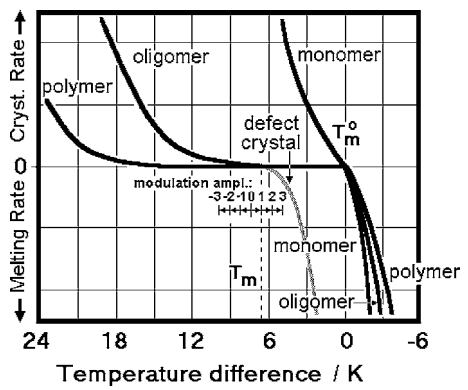

Fig. 6. Schematic plot of linear melting and crystallization rates as measured by microscopy on crystals of polyethylene, selenium, germanium oxide, phosphorous pentoxide, poly(oxymethylene), and poly(oxyethylene) of different molar masses [7]. Typical modulation amplitudes are indicated. The equilibrium melting temperature is T_m^0 and T_m represents the non-equilibrium melting of a defect crystal.

through a nucleation step before adding to a crystal, as was suggested almost 20 years ago [8].

The calorimetry used to obtain the data to be discussed, ranges from classical adiabatic calorimetry, needed for the measurement of low-temperature heat capacity shown in Figs. 2–4, to the standard DSC employed, for example, for the high-temperature data in Figs. 3–5, and the TMDSC required for the quasi-isothermal measurements in Fig. 5. Details about these three techniques can be found, for example, in lectures 19, 20, and 21, respectively, of the computer course on "Thermal Analysis of Materials" [1].

2. Melting of oligomers

Figs. 7 and 8 illustrate the irreversible melting of low and high molar mass polyethylene in the presence of higher-melting nuclei [9,10]. In both cases, there is a considerable supercooling between the observed melting and crystallization temperatures, as expected from Fig. 6. The supercooling changes little with the nature of the seeds, as illustrated in Fig. 7, and is time-dependent, as shown in Fig. 8.

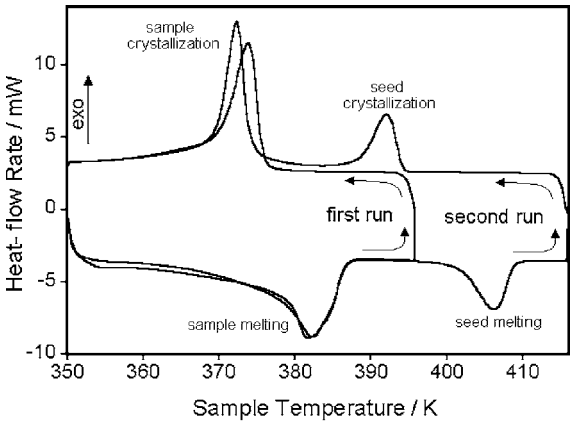

Fig. 7. Melting on heating, followed by crystallization on cooling of a polyethylene sample of molar mass 15,520 Da, seeded with high molar mass fibers [9]. Measured by DSC at 10 K min^{-1}. In the first run, the seeds did not melt. In the second run, the seeds melted and recrystallized at a higher temperature than the crystallization temperature of the samples of 15,520 Da mass. In neither case was there a reduction of the supercooling needed for crystallization.

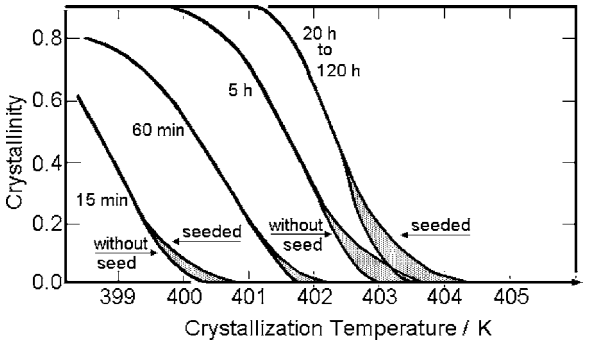

Fig. 8. Isothermal crystallization on cooling of polyethylene of a weight-average molar mass of 130,000 Da without and with seeds of extended-chain crystals of the same sample [10]. Measurements by DSC at 10 K min^{-1}, showing practically no reduction in supercooling due to the presence of the crystal nuclei. The equilibrium melting temperature of the seeds was 414.3 K, the melting temperature of the crystals was 7–9 K higher than the highest possible crystallization temperature. No crystallization occurred above 404.3 K.

A surprising observation was made when analyzing paraffins which are the oligomers of polyethylene. These short-chain, flexible molecules could not only melt and crystallize reversibly without supercooling, as illustrated in Fig. 9, but could also crystallize under many analysis conditions even without primary nucleation [11]. The agreement of the standard DSC and the quasi-isothermal TMDSC documents that the melting is reversible far into the melting range. At higher indicated temperatures the melting peak measured by standard DSC lags behind the TMDSC due

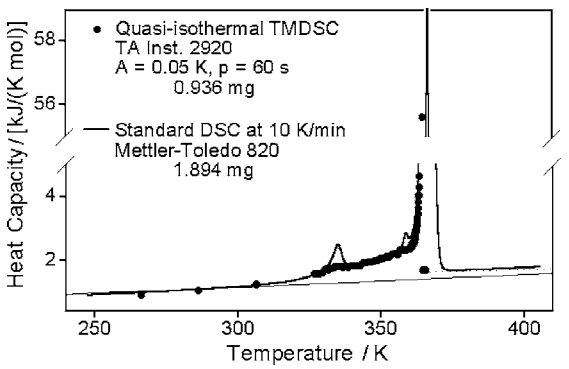

Fig. 9. Standard and quasi-isothermal DSC of pentacontane ($C_{50}H_{102}$) [11]. The thin line is the data bank value for the crystalline paraffin, and the dotted line, for the melt.

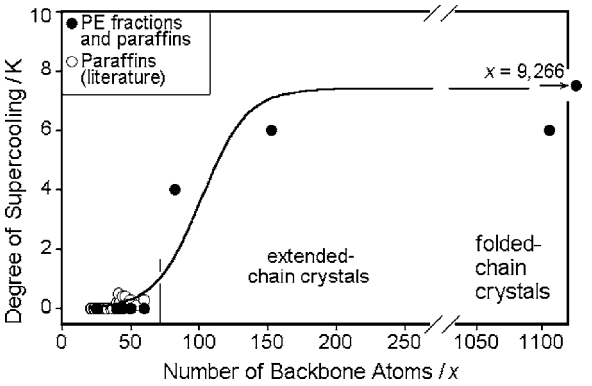

Fig. 10. Critical chain length for molecular nucleation of oligomers of polyethylene fractions (PE) and paraffins [11].

to insufficient heat conduction. A more detailed analysis by quasi-isothermal analysis revealed that for three types of flexible, linear molecules there exists a critical length of about 70 backbone atoms beyond which molecular nucleation is necessary under typical crystallization conditions [8]. Fig. 10 illustrates the data. The critical chain length is indicated by the vertical line in Fig. 10. The higher molar mass data represent the results of Figs. 7 and 8. The critical chain length of the oligomers seems to be independent of the macroconformations [7], i.e. whether the crystals contain extended-chain or folded-chain molecules.

These measurement suggest that oligomers of chain lengths shorter than the critical length can melt reversibly in a matrix of metastable, semicrystalline macromolecules. Furthermore, sufficiently short free chain ends may add to crystals of larger thickness or may form at low temperature their own crystals and in both cases melt reversibly. Even rather mobile interior parts of amorphous sections of macromolecules which are attached on both sides to crystalline nanophases may add reversibly to crystal surfaces of higher-melting crystals or form their own secondary crystals. Characteristically, these crystals melt close to the melting temperature of the corresponding oligomers, i.e. their melting occurs considerably lower than the temperature of the main melting peak. This low melting temperature is an indicator of the presence of such oligomer crystals.

In case the oligomer crystals are longer than the critical length, they would not melt reversibly, but they may still indicate reversing melting, i.e. a melting

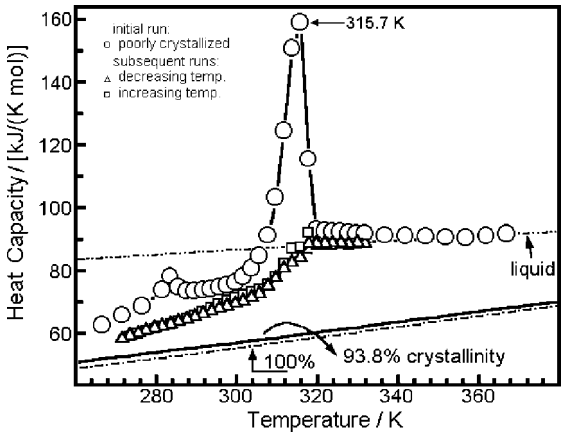

Fig. 11. Quasi-isothermal TMDSC of melting and crystallization for oligomeric poly(oxy-ethylene) of mass 1500 Da [12]. Sinusoidal modulation with an amplitude of 0.5 K and a period of 60 s. The heat capacities of the melt, the crystals, and a sample of 93% crystallinity, the value of the initial sample, are indicated as calculated from the ATHAS data bank [5].

based on non-equilibrium structures, as is indicated by the defect crystal in Fig. 6. Fig. 11 gives a typical example for POE of a mass of about 1500 Da (≈100 chain atoms). After fast crystallization, a small reversing melting peak is visible (○). On slow crystallization, the peak disappears almost completely (□), leaving only the increase in reversible C_p that is due to the conformational motion within the crystals,

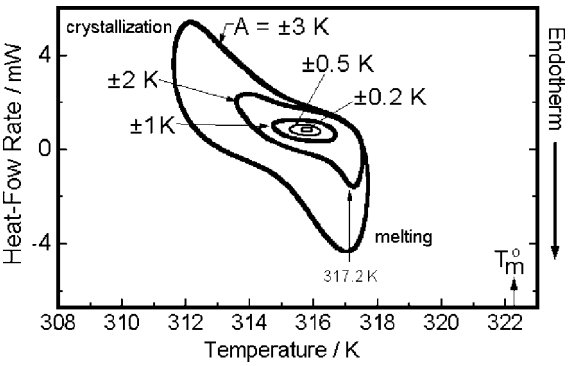

Fig. 12. Quasi-isothermal TMDSC of melting and crystallization for oligomeric poly(oxyethylene) of mass 1500 Da [12]. Sinusoidal modulation with the indicated amplitudes and a period of 60 s at 315.6 K. The data are plotted as Lissajous figures, clearly showing the different onsets of crystallization and melting making the process reversing and fitting the rates of melting and crystallization of the defect oligomer shown in Fig. 6.

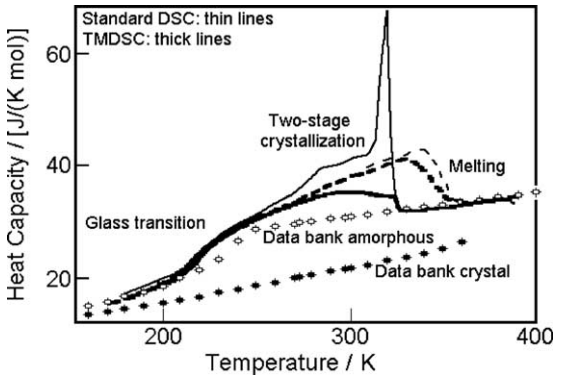

Fig. 13. Standard DSC and TMDSC of poly(ethylene-*co*-octene) of density 0.870 g cm^{-3} in the semicrystalline state [13]. Standard DSC with heating and cooling rates of 10 K min^{-1}, TMDSC with underlying heating and cooling rates of 1 K min^{-1} and a sinusoidal oscillation of the furnace using a period of 1.8 min and an amplitude of 1.0 K. Mettler–Toledo 820 DSC.

described in the previous section [12]. The supercooling can be judged by comparing the heating (□) and cooling (Δ) depicted in Fig. 11. Analyzing the Lissajous figures at different modulation amplitudes, as is depicted in Fig. 12, gives a more detailed picture as a function of time and temperature. Crystallization at amplitudes of 2 and 3 K leads to about the same initial crystallization temperatures, but to different melting behaviors because of the different times available for annealing. Further information could be gained by studies at different frequencies as well as amplitude.

3. Partially melted nanophase structures

Fig. 13 shows an analysis of a copolymer of ethylene with about 30 mass% octene-1 (≈10 mol%) [13], a linear, low-density polyethylene of high regularity, produced by co-polymerization using a metallocene catalyst. Following various experiments, one can see that in the low-temperature region of the crystallization and melting the transition is increasingly reversing. This is most likely caused by amorphous portions of the backbone chain of a length equivalent to sub-critical oligomers, giving a fringed-micellar structure. Fig. 14 illustrates the equivalence of the melting temperatures of paraffins with isotactic polymers with side-chains of equivalent lengths [14]. For atactic polymers the crystallizing portion is only that

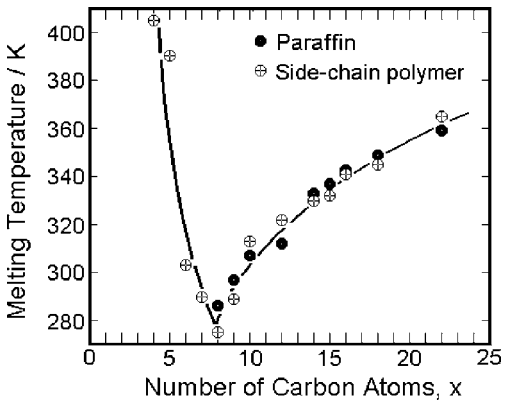

Fig. 14. Melting temperatures of isotactic side-chain vinyl polymers and the corresponding paraffins [7,14]. Formulae: Polymer $[CH_2–CH(C_{x-2}H_{2x-3})–]_n$, paraffin $C_{2x}H_{4x+2}$.

of the side-chain [7], so that from 250 to 350 K, the equivalent paraffin crystals would range from about 11 to 42 chain atoms, i.e. be shorter than the critical chain length derived from Fig. 10. The higher-melting crystals grow mainly during the primary crystallization which is characterized by the sharp crystallization peak in Fig. 13. These crystals melt largely irreversibly. The quasi-isothermal TMDSC in this high-temperature region reveals a substantial amount of slow annealing which contributes to the reversing heat capacity [13]. Fig. 15 shows the change of the reversing heat capacity in a quasi-isothermal experiment as a function of time at 299 K. Extrapolating to infinite time, there is still a reasonable latent heat contribution to the apparent heat capacity left, which cannot be formed by sub-critical oligomer-length chain segments. In this case, one must assume that on the growth-face for crystallization, incomplete melting occurs which is also reversible on a molecular level. This concept involves the molecular nucleation proposed a number of years ago [8] to explain the metastable region of the polymer melt between the crystallization and melting temperatures shown in Fig. 6. Once melted, a polymer molecule is assumed to undergo a molecular nucleation process for recrystallization which involves a free enthalpy barrier caused by the need to reduce the entropy of the crystallizing molecule by reorientation to a more stretched conformation before gaining the full latent heat of fusion. Melting should thus be reversible on a molecular scale, but only as long as there is a remaining crystalline portion or configuration which can serve as a molecular nucleus (i.e. crystallization without a free energy barrier). Once the molecule is completely melted, supercooling is necessary to overcome the activation energy of nucleation, as is indicated by the experiments of Figs. 7 and 8. The concept of such reversible melting at temperatures which exceed the chain segments of critical length is illustrated in the schematic of Fig. 16. Within the metastable network of crystals of the global structure, one can thus identify reversible, local equilibria. Combining the details

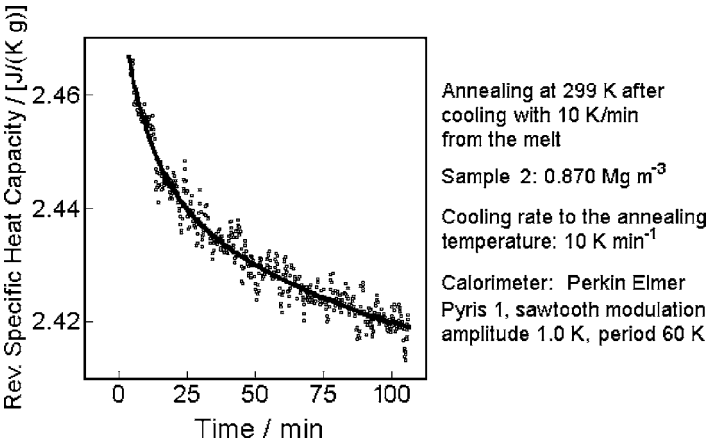

Fig. 15. Change of the reversing heat capacity on quasi-isothermal TMDSC of the sample of Fig. 13 at 299 K after cooling from the melt at 10 K min^{-1} [13].

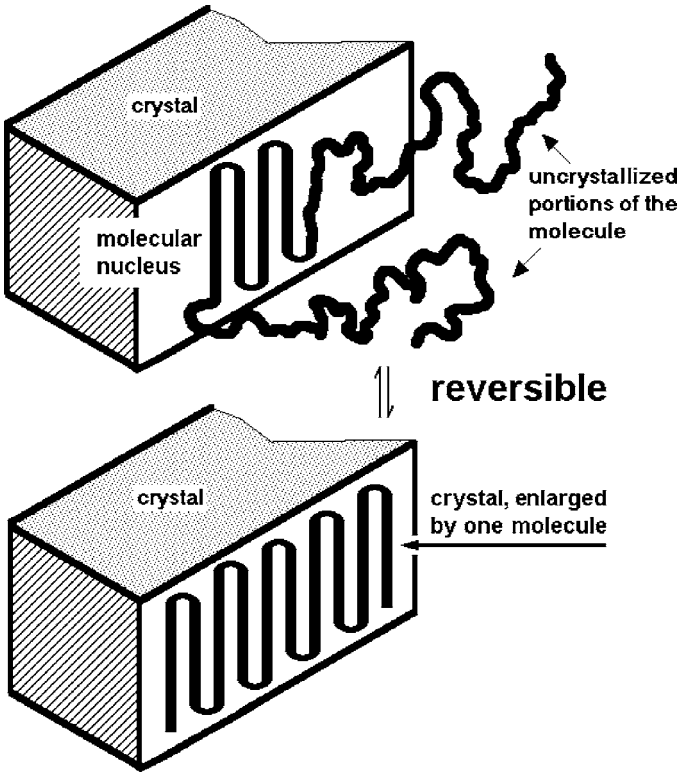

Fig. 16. Schematic of partial, reversible melting with a remaining molecular nucleus.

of the structure (by X-ray diffraction), mobility (by solid state NMR) and reversibility as a function of frequency and amplitude (by TMDSC), it may be possible to gain much more insight into the nanophase structure of semicrystalline polymers.

4. Conclusions

The vibrational contributions to C_p are reversible up to very fast times, as illustrated in Fig. 2. Additional large-amplitude motion can increase C_p to the level of the liquid and is also reversible as long as the motion is not cooperative. A latent heat is connected to changes in the phase structure which are cooperative and, thus, usually much slower than the heat capacity contribution from vibrations and isolated conformational motion. The measured C_p is then an apparent heat capacity, $C_p^{\#}$, and needs to be separated into its different contributions for a more detailed discussion.

Due to the nanophase structure of semicrystalline polymers, local equilibria exist which give reversible contributions, but may be masked by slow reorganization and annealing, as shown in Fig. 15. Chains or chain segments of less than the critical size indicated in Fig. 10 can melt reversibly as long as the metastable, overall phase structure remains unchanged. Finally, the molecular nucleation, as illustrated in Fig. 16, can explain a small amount of reversible melting of parts of molecules on the growth-face of the crystal. It is based on a mechanism that involves only parts of molecules. Once a molecule is completely melted, the reversibility does not exist anymore.

In the flexible molecules, like polyethylene, there may be a third mechanism which involves a sliding diffusion of defects through the crystals. It is based on the beginning of large-amplitude motion in the form of the *gauche-trans* conformations described above, and was also seen in molecular dynamics simulation of the polymer crystals [15]. The increase in the number

and mobility of the defects may result in a reversible, temperature-dependent reorganization of the fold surface, which has also been labeled a reversible melting [16], although it may not involve an actual phase transition, but only a reversible change in the surface structure.

Overall, one can thus distinguish three reversible processes which may involve additional latent heats: (i) The conformational motion of large-amplitude, that increases the heat capacity beyond the baseline of the vibrational contribution shown in Figs. 2–4 and may lead to changes in the interface structure. (ii) The melting of small segments of macromolecules (or oligomers) below a critical length, as suggested by Fig. 10. (iii) The melting of long segments of macromolecules which have a melting temperature within the main melting peak, but need no molecular nucleation due to partial melting, as indicated in Fig. 16.

It must finally be remarked that the present discussion is concentrating on polyethylene. Other polymers have different values for the three enumerated contributions. Methylene chains show, for example, a particularly large contribution to $C_p^{\#}$ because of a large potential energy contribution on the change between its two conformational isomers. Phenylene-containing chains, in contrast, contain almost no heat capacity effect because of the high symmetry of ring flips about the chain axis which is also active below the melting temperature. For homopolymers, contributions from the short-chain segments become much smaller than shown in Fig. 13.

Acknowledgements

The work was supported by the Division of Materials Research, National Science Foundation, Polymers Program, Grant #DMR-9703692 and the Division of Materials Sciences and Engineering, Office of Basic Energy Sciences, US Department of Energy at Oak Ridge National Laboratory, managed and operated by UT-Battelle, LLC, for the US Department of Energy, under contract number DOE-AC05-00OR22725.

References

[1] Thermal Analysis of Materials, downloadable: http://web.utk.edu/~athas/courses/tham99.html.
[2] B. Wunderlich, Thermochim. Acta 300 (1997) 43.
[3] B. Wunderlich, M. Pyda, J. Pak, R. Androsch, Thermochim. Acta 377 (2001) 9.
[4] Y. Jin, B. Wunderlich, J. Phys. Chem. 95 (1991) 9000.
[5] B. Wunderlich, The ATHAS data base on heat capacities of polymers, Pure Appl. Chem. 67 (1995) 1919 (for data see: http://web.utk.edu/~athas).
[6] I. Okazaki, B. Wunderlich, Macromolecules 30 (1997) 1758.
[7] B. Wunderlich, Macromolecular Physics, vol. 2, Crystal Nucleation, Growth, Annealing, vol. 3, Crystal Melting. Academic Press, New York, 1976, 1980.
[8] B. Wunderlich, A. Mehta, J. Polym. Sci., Polym. Phys. 12 (1974) 255;
B. Wunderlich, A. Mehta, Colloid. Polym. Sci. 253 (1975) 193.
[9] J. Pak, Thesis, Department of Chemistry, University of Tennessee, 2001.
[10] B. Wunderlich, C.M. Cormier, J. Phys. Chem. 70 (1966) 1844.
[11] J. Pak, B. Wunderlich, J. Polym. Sci., Part B: Polym. Phys. 38 (2000) 2810;
J. Pak, B. Wunderlich, Macromolecules 34 (2001) 4492.
[12] K. Ishikiriyama, B. Wunderlich, Macromolecules 30 (1997) 4126;
K. Ishikiriyama, B. Wunderlich, J. Polymer Sci., Part B, Polym. Phys. 35 (1997) 1877.
[13] R. Androsch, B. Wunderlich, Macromolecules 32 (1999) 7238;
R. Androsch, B. Wunderlich, Macromolecules 33 (2000) 9076.
[14] G. Trafara, R. Koch, K. Blum, D. Hummel, Makromol. Chem. 177 (1976) 1089.
[15] B.G. Sumpter, D.W. Noid, G.L. Liang, B. Wunderlich, Adv. Polym. Sci. 27 (1994) 116.
[16] W. Hu, Th. Albrecht, G. Strobl, Macromolecules 32 (1999) 754.